

Efficient time stepping for numerical integration using reinforcement learning

Michael Dellnitz¹, Eyke Hüllermeier², Marvin Lücke³, Sina Ober-Blöbaum¹, Christian Offen¹, Sebastian Peitz⁴, and Karlson Pfannschmidt⁴

¹*Department of Mathematics, Paderborn University*

²*Department of Computer Science, LMU Munich*

³*Modeling and Simulation of Complex Processes, Zuse Institute Berlin*

⁴*Department of Computer Science, Paderborn University*

Abstract

Many problems in science and engineering require the efficient numerical approximation of integrals, a particularly important application being the numerical solution of initial value problems for differential equations. For complex systems, an equidistant discretization is often inadvisable, as it either results in prohibitively large errors or computational effort. To this end, adaptive schemes have been developed that rely on error estimators based on Taylor series expansions. While these estimators a) rely on strong smoothness assumptions and b) may still result in erroneous steps for complex systems (and thus require step rejection mechanisms), we here propose a data-driven time stepping scheme based on machine learning, and more specifically on reinforcement learning (RL) and meta-learning. First, one or several (in the case of non-smooth or hybrid systems) base learners are trained using RL. Then, a meta-learner is trained which — depending on the system state — selects the base learner that appears to be optimal for the current situation. Several examples including both smooth and non-smooth problems demonstrate the superior performance of our approach over state-of-the-art numerical schemes. The code is available under <https://github.com/lueckem/quadrature-ML>.

1 Introduction

The numerical treatment of a vast number of problems in science and engineering requires the approximation of integrals, such as the computation of volume or mass flow or the numerical solution of differential equations via *Runge–Kutta methods* [3]. Consequently, schemes for numerical discretization are a key element of scientific computing, and one of the main challenges is to determine a good trade-off between the required accuracy and numerical efficiency.

While the standard approach to developing *quadrature rules* is based on Taylor series expansions and the associated error bounds determined by higher-order derivatives [3], the advances in data science and machine learning have recently fueled the development of alternative concepts that are based on *training data*. Most of these approaches are developed with the aim to efficiently compute the numerical solution of complex dynamical systems, see, for instance, [19, 26, 16, 20, 21, 13], where the flow map F that takes a state x at time t to a future state $x(t + \Delta t)$ is approximated.

In contrast to that, our work addresses the task of efficiently performing numerical quadrature for arbitrary, explicitly known functions. To this end, the next sample point at which the function is evaluated is determined by finding an *optimal trade-off* between the two conflicting criteria accuracy and numerical efficiency. This task is carried out by a *reinforcement learning* algorithm which, taking past function evaluations into account, determines the next sample point at which to evaluate the function of interest. As many practical problems involve rapid changes or even non-smoothness, the training of just one time-stepper will likely lead to an overall mediocre performance. To circumvent this, a *hierarchical approach* (Section 3) is pursued, where multiple *base learners* (Section 3.1) are trained to yield a very good performance on subsets with a specific structure or behavior. Based on recent function evaluations, an additional *meta-learner* (Section 3.2) then chooses the appropriate base learner to perform the time-stepping. The efficiency of the proposed approach in comparison to state-of-the-art methods will be

demonstrated using both examples from the area of integrating functions as well as numerically solving of differential equations (Section 4).

While our method requires explicit knowledge of the function of interest, its applicability is not limited to dynamical systems, but also applies to the calculation of integrals. To address unknown systems, methods for system identification from data can be employed, which have been increasingly popular in recent years (cf., e.g., [2, 22, 13]).

Finally, the second key component of quadrature rules—the appropriate weighting of the different function evaluations—will be addressed briefly in Section 5. Besides the classical Taylor-series-based construction (e.g., via the Newton-Cotes formulae), these weights can also be determined from data using regression techniques.

2 Preliminaries

We will now briefly introduce the main task this paper addresses—the numerical approximation of integrals—and then draw a connection to numerical algorithms for differential equations. Finally, we give a brief overview over the reinforcement learning framework we will use in our algorithm.

2.1 Numerical Quadrature

The task in numerical quadrature is to efficiently determine the value of the integral

$$I = \int_a^b f(x)dx \tag{1}$$

from a few function evaluations $f(x_i)$ at s distinct positions x_1, \dots, x_s , while maintaining a high accuracy. The most wide-spread strategy is to divide the interval $[a, b]$ into subintervals $[a_i, a_{i+1}]$ of length Δ and to apply a quadrature formula

$$I_i = \sum_{j=1}^n \omega_j f(a_i + c_j \Delta), \tag{2}$$

with fixed nodes $0 \leq c_1 < \dots < c_s \leq 1$ and weights $\omega_j \in \mathbb{R}$ in each subinterval. Such quadrature formulae—i. e., a specific choice of nodes and weights—are based on Taylor series expansions. If an odd number of equidistant nodes are given, then the weights c_i can be computed such that the approximation is of order $s + 1$ (Newton-Cotes formula). For tailored choices of quadrature nodes, Gauss-Legendre quadrature formulae achieve order $2s$ [4].

In contrast to fixed subintervals and quadrature rules, adaptive methods use problem specific data to cluster nodes in rapidly changing regions of the integrand f and to minimize evaluations elsewhere. In classical Romberg quadrature [4], the value of the integral on the subinterval is computed by first calculating a sequence of approximations using quadrature rules of increasing order. New approximations are obtained efficiently by combining prior approximations until an estimated error is sufficiently small. Should the highest available order not yield a sufficiently accurate solution, then the corresponding subinterval is further subdivided into two intervals of half the size. This process is repeated until the desired accuracy is reached.

2.2 Numerical integration of differential equations

We now would like to approximate the solution x of an initial value problem $\dot{x} = f(t, x)$ with initial condition $x(t_0) = x_0$ on the time interval $[t_0, t_1]$. Reformulating the initial value problem as

$$x(t_1) = x_0 + \int_{t_0}^{t_1} f(t, x(t))dt, \tag{3}$$

reveals a relation to (1). Numerical quadrature then gives rise to integration methods for ordinary differential equations such as *Runge-Kutta* methods. Time-stepping proceeds as follows: for a given step size $h_0 > 0$, first the approximate value x_1 of the solution $x(t_1)$ at time $t_1 = t_0 + h_0$ is computed. Next, the process is repeated with (t_1, h_1, x_1) replacing (t_0, h_0, x_0) to compute x_2 for $h_1 > 0$. Iteration yields an approximation x_0, x_1, x_2, \dots of the solution x at times t_0, t_1, t_2, \dots , where $t_j = t_{j-1} + h_{j-1}$ is recursively defined.

While in the simplest case all step sizes h_j are identical (constant time-stepping), more elaborate schemes choose step sizes dynamically based on error estimates that are available from previous steps. In this way, numerical integration can benefit from large time steps in regions where the solution does not change rapidly while satisfying accuracy requirements in regions which require small step sizes [10, 9]. Efficient time-stepping methods that are implemented in MATLAB or Python’s Scipy package [29] include most prominently the Dormand–Prince pair RK45, consisting of a fifth order Runge–Kutta scheme together with a fourth order method that is used to estimate the local error of each step. Based on the error estimate, a step-size controller then computes the step-size for the next iteration [5, 25]. Other methods include the 8th order scheme DOP853 [10, 24], or multi-step strategies for stiff equations [10] as well as automatic solver selection strategies [31].

The above-mentioned black box solvers are designed for an application to a broad range of problems. However, for problems with additional structure (for instance, Hamiltonian systems), specialized algorithms achieve significant advantages over off-the-shelf methods by making use of symmetries, conserved quantities, or symplecticity [8]. On the other hand, a lack of regularity of problems can cause order reductions or instabilities of classical integration schemes that are hard to overcome, though approaches are available in some cases [14].

2.3 Reinforcement and meta-learning

While specialized schemes have traditionally been developed by manually identifying structures first and then designing appropriate numerical schemes, in the following we will explore a data-driven approach to develop time-stepping strategies tailored to given problem classes. In our approach, these strategies are learned by a neural network for specific problem classes such as integrands with discontinuities. In comparison to classical adaptive schemes, the neural network can learn features specific to the problem class and use that knowledge to optimize its time-stepping strategy. Depending on the current system state, a meta-learner can then select from a set of such *base learners* to address a large class of systems, including hybrid models with qualitative changes in behavior.

2.3.1 Reinforcement learning

In reinforcement learning, we consider an agent acting in an environment E , typically modelled in the form of a Markov decision process $(\mathcal{S}, \mathcal{A}, p, r)$, with \mathcal{S} the set of possible states, \mathcal{A} the set of possible actions, p the so-called transition function, and r the reward function. At each discrete time step t , the agent finds itself in a state $s_t \in \mathcal{S}$ of the environment. It decides on an action $a_t \in \mathcal{A}$ and receives an immediate reward $r_t = r(s_t, a_t) \in \mathbb{R}$ that depends on the current state and the action taken (and perhaps also on the successor state). The behavior of the agent is captured by its *policy* $\pi: \mathcal{S} \rightarrow P(\mathcal{A})$ that prescribes actions given states. More specifically, the policy is not necessarily deterministic and defines a probability distribution over the actions available in a given state. Likewise, the environment can be stochastic: The successor state s_{t+1} resulting from action a_t in the current state s_t , is determined by the transition function $p: \mathcal{S} \times \mathcal{A} \rightarrow P(\mathcal{S})$. In the following, we will use the notation $r_t, s_{t+1} \sim E$ as a shorthand whenever s_t and a_t are clear from the context.

Given a sequence of states and actions $(s_t, a_t, s_{t+1}, a_{t+1}, \dots, s_T)$ starting at state s_t , an important quantity is the sum of discounted future rewards $R_t = \sum_{i=t}^{T-1} \gamma^{(i-t)} r(s_i, a_i)$, where $\gamma \in [0, 1]$ is a discount factor. The actions are the result of sampling from the (stochastic) policy π , which is not known in advance. The challenge thus becomes to learn a policy which, given an initial state $s_0 \in \mathcal{S}$, maximizes the *expected* sum of discounted future rewards.

Here it is useful to consider the expected future rewards with respect to a specific action. The action-value function is defined as follows:

$$Q^\pi(s_t, a_t) = \mathbb{E}_\pi[R_t \mid s_t, a_t] \quad (4)$$

It assumes that the agent picks action a_t in state s_t , while subsequently picking actions according to policy π . This definition can be further unrolled into a recursive definition:

$$Q^\pi(s_t, a_t) = \mathbb{E}_{r_t, s_{t+1} \sim E}[r(s_t, a_t) + \gamma \mathbb{E}_{a_{t+1} \sim \pi}[Q^\pi(s_{t+1}, a_{t+1})]] \quad (5)$$

This equation is known as the Bellman equation [15, 27]. Note that the outer expectation is not needed in case of a deterministic environment, while the same holds for the inner expectation for a deterministic

policy function. We will call the function

$$Q(s_t, a_t) = \mathbb{E}_{r_t, s_{t+1} \sim E} \left[r(s_t, a_t) + \gamma \max_{a_{t+1} \in \mathcal{A}} Q(s_{t+1}, a_{t+1}) \right], \quad (6)$$

which evaluates the action a_t in state s_t based on the premise that optimal actions are chosen in subsequent steps, the *Q-function*. Thus, the optimal policy $\pi^*: \mathcal{S} \rightarrow \mathcal{A}$ can be characterized as

$$\pi^*(s) = \arg \max_{a \in \mathcal{A}} Q(s, a). \quad (7)$$

In this paper we use a reinforcement learning approach based on Q-learning [30], where the *Q-function* is approximated by a neural network parametrized by θ . In the beginning θ is initialized using a suitable initialization scheme [7]. The training then proceeds over the course of several episodes. In each episode the learner starts in state $s_0 \in \mathcal{S}$ of the environment and explores the state space using the function Q_θ in conjunction with a probabilistic policy. This results in a trajectory $((s_t, a_t, r_t))_{t=0}^H$, where s_t is the state in time step t , a_t the chosen action, and r_t is the resulting reward. The horizon H is the final time step of the trajectory and marks the end of one episode. The training targets Q'_θ are defined as follows:

$$Q'(s_t, a_t) = r_t + \gamma \max_{a \in \mathcal{A}} Q_\theta(s_{t+1}, a). \quad (8)$$

Given a loss function $L: \mathbb{R} \times \mathbb{R} \rightarrow \mathbb{R}$, the parameter vector $\hat{\theta}$, to be used in the next episode, is calculated using empirical risk minimization:

$$\hat{\theta} \leftarrow \arg \min_{\theta \in \Theta} \frac{1}{H+1} \sum_{t=0}^H L(Q'(s_t, a_t), Q_\theta(s_t, a_t)) + R(\theta), \quad (9)$$

where $R(\theta)$ is an additional regularization term. In the following we use the typical L_2 loss, i. e., $L(y, \hat{y}) = \|y - \hat{y}\|_2$. We continue to run episodes until the *Q-function* converges. This approach (and similar variants) is often referred to as *deep Q-learning* [17]. While convergence to the exact *Q-function* is only rigorously proven for classical Q-learning in a finite state and action space setting [11], there are numerous publications showing the success of deep Q-learning in many applications. For an overview, the reader is referred to [6].

2.3.2 Meta-learning

As previously mentioned, optimal time-stepping strategies vary depending on the problem class at hand. While reinforcement learning can be utilized to optimize a time-stepping strategy for one given task, the question arises, whether a meta-strategy can be learned, which decides on the most appropriate strategy from a set of available ones. Questions of this type are typically tackled using techniques from *meta-learning* [23]. In the general formulation, it is assumed that learning tasks T are generated by a distribution $P(\mathcal{T})$. The learner is able to observe M tasks $\{T_i\}_{i=1}^M$ and the associated data sets. The goal then is to quickly and accurately adapt to unseen tasks $T \sim P(\mathcal{T})$. For this paper, we assume that the learner has access to a diverse set of problem classes from which target functions can be sampled. We consider each of these problem classes as one particular task. While the general meta-learning setting treats each task as separate, we also want to be able to deal with abrupt changes in the target function. As another important difference, we note that meta-learning typically seeks to adapt model parameters at test time, whereas here we consider the learners and the meta-learner to be fixed.

3 A hierarchical RL algorithm for optimal time stepping

Our algorithm addresses two main challenges of numerical integration schemes:

- (i) the selection of step sizes in situations of rapidly changing behavior (e. g., bursts),
- (ii) qualitative changes in behavior, for instance in hybrid or switched systems.

Our approach to the first issue is to train one (or, depending on the system, multiple) *base learners* that are superior to classical schemes based on quadrature. This allows us, in particular, to address issues such as the use of too large step sizes (“overshooting”) at points where dynamics change rapidly. The second issue is tackled by a meta-learning approach. At each time instance, a meta-learner selects — depending on the system state — the optimal time stepper from a set of base learners.

3.1 Training of base learners via reinforcement learning

We aim to counter the phenomenon of “overshooting” by using a neural network (NN) to predict a good next step size. We assume that the functions we want to integrate are sampled from a set X with probability measure P . Provided with a sufficient amount of training data, the NN should be able to predict the future course of the function to some extent and, thus, choose a suitable time step¹.

To this end, we construct an algorithm of order two, i. e., using three function values per step¹. In every integration step, we provide the model with the 3 evaluations $f(x_1), f(x_2), f(x_3)$, where the step size is given as $h = x_2 - x_1 = x_3 - x_2$. Based on this input, the model chooses the step size for the next integration step $h^+ \in \{h_1, \dots, h_n\}$ from a finite set of possible options. For the approximation of the integral, we use the standard Simpson rule for now. The optimal step size is chosen by an NN trained via Q-learning [30]. More specifically, the NN approximates the Q-function, where Q receives the *state* s_t at time t and an *action* a_t as inputs which, in our case, are

$$\begin{aligned} s_t &= (h, f(x_1), f(x_2), f(x_3)), \\ a_t &= h^+. \end{aligned}$$

From the tuple (s_t, a_t) we can calculate the state in the following integration step as

$$s_{t+1} = (h^+, f(x_3), f(x_3 + h^+), f(x_3 + 2h^+)).$$

As described above, the value of the Q-function can be defined implicitly as

$$Q(s_t, a_t) = r_t + \gamma \max_{a_{t+1} \in \mathcal{A}} Q(s_{t+1}, a_{t+1}),$$

with reward r_t and discount factor $\gamma \in (0, 1)$. The neural network receives s_t as an input and returns all possible Q-values, i. e., the output is defined as

$$(Q(s_t, h_1), \dots, Q(s_t, h_n)).$$

We then simply choose the action with the highest Q-value, i. e., the highest expected reward, as our next step size. In the following numerical examples in section 4, the training of the neural network was conducted as described in equation (8).

In order to achieve our goal, namely choosing a step size that is as large as possible while an error tolerance tol is not exceeded, we have to choose an appropriate reward function. In our case the reward r_t should depend on the integration error ε in the integration step t and on the chosen step size h . A straightforward approach is

$$r_t = \begin{cases} 0, & \varepsilon > \text{tol} \\ h, & \varepsilon < \text{tol} \end{cases}.$$

However, in practice it is advantageous to use a reward function with negative rewards for larger errors. To this end, one can use the following reward function:

$$r_t = \begin{cases} ae^{-b\varepsilon} - L, & \varepsilon > \text{tol} \\ \frac{h}{h_n}, & \varepsilon < \text{tol} \end{cases}, \quad (10)$$

where a, b and L are tuning parameters. For example, these parameters could be chosen such that $r_t = 0$ if $\varepsilon = \text{tol}$, $r_t = -1$ if $\varepsilon = 2 \text{ tol}$ and $r_t \approx -3 = -L$ if the error ε is very large. We additionally scale the positive rewards by dividing by the largest possible step size, so that the reward is bounded by one. In general, it is a good idea to keep the positive and negative range of the rewards balanced (e. g., bounded by $[-5, 5]$), so that the resulting model is balanced. If we chose a reward function with strongly negative rewards for large errors but only small positive rewards, for example, then the resulting model might be overly conservative and cautious.

It should be noted that our choice of a reward function is still not continuous, which could impact the learning time. To solve this problem, one could for example use

$$r_t = \frac{h}{h_n} (ae^{-b\varepsilon} - L),$$

¹It should be noted that the extension to models of higher order is straightforward by increasing the number of inputs to the neural network. For order three, numerical tests show very similar behavior to the one observed for order two.

where negative and positive rewards are scaled by the chosen step size. If the errors are expected to be scattered over a wide range, for instance if there is a discontinuity that results in errors multiple orders larger than elsewhere, the reward functions presented above might not work that well. The reason is that for errors multiple orders larger than the tolerance, we always have $r_t \approx -L$ and thus, a smaller error does not increase the reward by much. Therefore, we can choose the following reward function in these cases:

$$r_t = \begin{cases} \log_{10}(\frac{\text{tol}}{\varepsilon}), & \varepsilon > \text{tol} \\ \frac{h}{h_n}, & \varepsilon < \text{tol} \end{cases},$$

which generates a reward of $r_t = -m$ if $\varepsilon = 10^m \cdot \text{tol}$. In summary, the problem of finding a good reward function is quite difficult and might need to be adapted for different function classes.

Throughout this paper, we use fully connected neural networks with four hidden layers and five times the number of input nodes per hidden layer. It should be noted that for the examples studied in the following, a significantly smaller network topology might be sufficient. All NNs use rectified linear unit (ReLU) activation functions, and employ the Adam stochastic gradient descent optimizer [12] for training.

Finally, we standardize the input data for the NN to render the learning independent of the absolute values of the function f . More precisely, instead of using the states $s_t = (h, f(x_1), f(x_2), f(x_3))$ as mentioned earlier, we use the centered versions $s_t = (h, f(x_2) - f(x_1), f(x_3) - f(x_1))$. With this approach, some information about the function values is lost. However, this disadvantage is compensated by the advantage that the resulting model is also applicable to translated functions $f + \text{const}$.

3.2 Meta-learning for the selection of various base learners

As mentioned above, there are several approaches on how to design a meta-learner that selects the base learner best suited for the current situation. In order to avoid constructing another neural network architecture, we will here use the same Q-learning approach as above, meaning that we determine the reward for choosing a specific base learner as the Q-value this learner receives after making its step size selection. Hence, we first train a set of base learners, and then perform a second reinforcement learning procedure for the meta-learner once the base learners have finished training.

4 Results

Before we address the main area of application, i.e., the numerical solution of differential equations, we will study the properties of our approach on smooth and non-smooth quadrature tasks.

4.1 Numerical quadrature

Our first test is to approximate integrals for a class of smooth functions composed of five superposed sine functions, i. e.,

$$X = \left\{ f : f(x) = \sum_{i=1}^5 c_i \sin(\omega_i x + \varphi_i) \mid c_i, \omega_i, \varphi_i \in \mathbb{R} \right\} \quad (11)$$

with probability measure $c_i \sim \text{Unif}[0, 1]$, $\omega_i, \varphi_i \sim \text{Unif}[0, 2\pi]$. Here we only study the performance of a single base learner. As the set of step sizes, we choose $\{0.05, 0.1, 0.15, 0.2, 0.3, 0.4, 0.5, 0.75\}$, and the error tolerance is set to $\text{tol} = 0.0005$. For the base learner training, we repeatedly sample functions from the proposed class (11) and use the step sizes suggested by the model. In the setting of quadrature, we are particularly interested in maximizing the immediate reward, i. e., choosing the best possible step size for the next step. Thus, we typically set the discount factor γ to small values or even to zero, in which case the Q-function collapses to

$$Q(s_t, a_t) = r_t.$$

Hence, during the training process we optimize the weights of the NN such that the outputs represent the expected immediate reward for all step sizes. For a good exploration of policies, we found it to be sufficient to simply choose the step size with the highest suspected reward with a fixed probability $\alpha \geq 0.5$ and the second highest with probability $1 - \alpha$. We use (10) as the reward function, and the error

is calculated by comparing with standard quadrature with very small step sizes, which we assume to be the ground truth.

An example application of the trained model can be seen in Figure 1. We see that the step size selection appears to be satisfactory in most places, but that the error bound is violated in a few time steps as well. This can either be circumvented by a stronger penalization of violating the tolerance, or by improving the prediction accuracy. Motivated by the fact that additional measurements allow us to approximate higher-order derivatives (e. g., the curvature) via Taylor expansions, a first approach to improve the performance is to add delayed measurements to the model, i. e., to extend the input by previous states. We say the model has a *memory* of m , if it can access the current state and m previous states. However, it should be noted that increasing the model’s memory results in additional complexity which can increase training times and training data requirements. Furthermore, m additional time steps are required when first initializing the integrator.

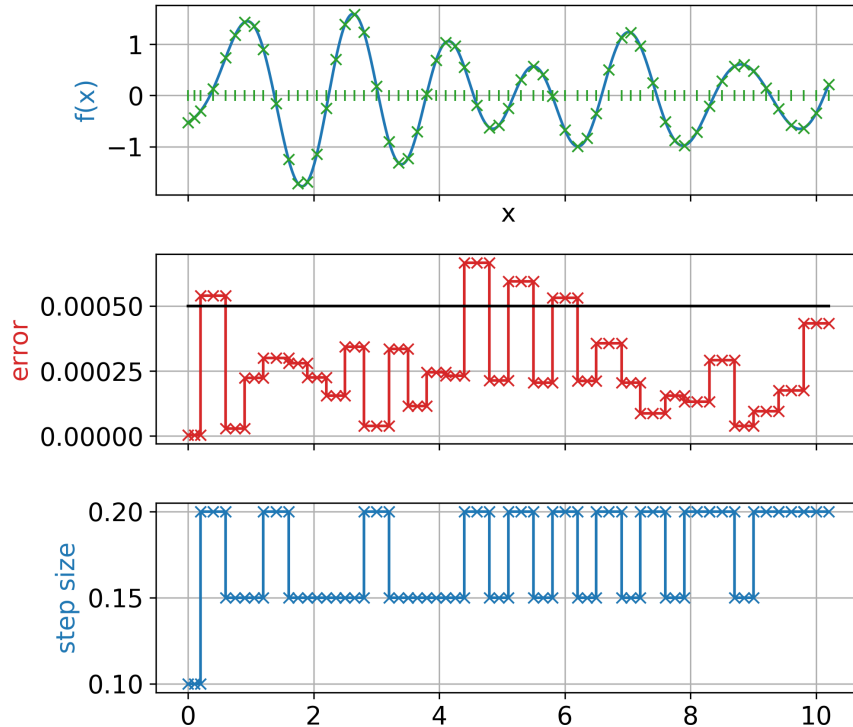


Figure 1: Integration of a function from the class (11) using the trained base learner.

To compare the integrator with classical methods, we examine the average integration error per integration step and the average number of steps required to integrate functions over the range $[0, 20]$ over a random sample of 5000 functions from the class (11). As Romberg quadrature of fixed order two performs poorly on sine functions (due to the aforementioned overshooting), we will disregard it and only compare the model to the equidistant composite Simpson rules with different time steps and to a subdivision algorithm with different numbers of maximum function evaluations (thereby limiting the number of subdivision steps).

The subdivision algorithm works as follows: denote by $s_f(a, b)$ the Simpson rule evaluated on the interval $[a, b]$, i. e., $s_f(a, b) = \frac{b-a}{6}(f(a) + 4f(\frac{a+b}{2}) + f(b))$. The subdivision algorithm constructs a rough estimate $I_r = s_f(a, b)$ of the integral on an interval $[a, b]$ and a fine estimate $I_f = s_f(a, \frac{a+b}{2}) + s_f(\frac{a+b}{2}, b)$. The difference $I_r - I_f$ is then an estimator for the integration error [4]. The subdivision algorithm iteratively identifies the interval with the highest estimated error and divides that interval at its center into two subintervals until a given number of maximum function evaluations is reached.

The results for the five superposed sine functions are plotted in Figure 2a, and we observe almost identical performance. However, a small improvement for the class (11) can be achieved when increasing the memory m . The reason why the performance is not superior is most likely that the class (11) is already quite complex, so that predictions of future function values are not feasible. Thus, the step size

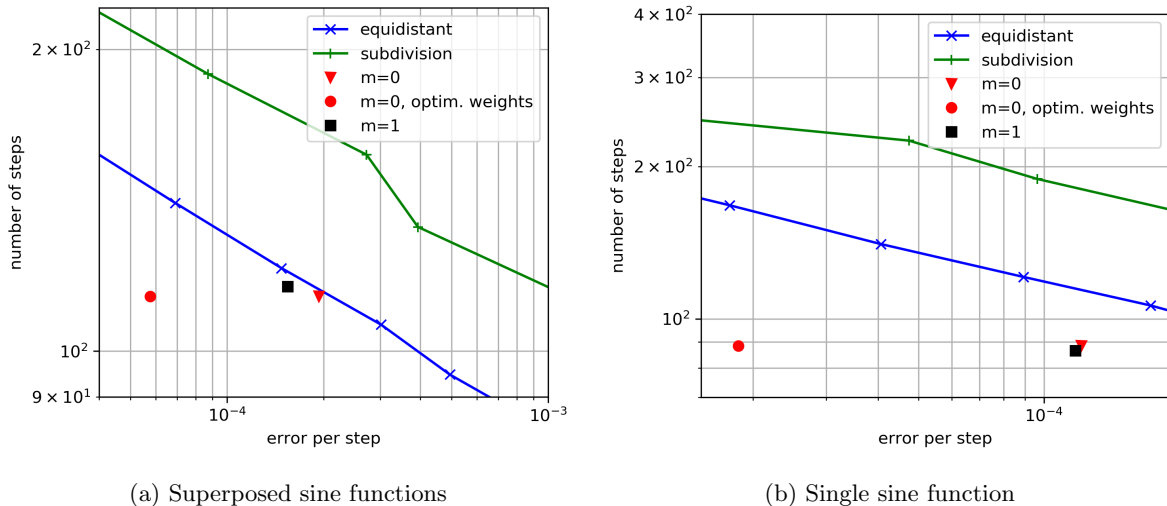


Figure 2: (a) Performance of the model with a memory of $m = 0$ and $m = 1$, respectively, and the equidistant composite Simpson rules for integrating functions of the class (11) from 0 to 20. The blue and green lines show the standard quadrature on equidistant and adaptive grids, respectively, with different step sizes. In addition, the potential of optimizing the weights (cf. Section 5) is shown. (b) The same comparison for a single sine function.

control is not beneficial in comparison to choosing equidistant nodes. In fact, the model tends to only select one of the two step sizes 0.15 and 0.2, which supports the assumption that the function class is too complex for systematically exploiting patterns. Thus, in expectation an almost equidistant time stepping is advisable and comparable to the equidistant composite Simpson rule with step size ≈ 0.17 . In contrast, when comparing the approaches on sine functions only (cf. Figure 2b), our approach clearly outperforms the classical quadrature.

We suspect that this behavior applies more generally: As the function class gets more versatile and predictions become more difficult, the model tends to always pick the same step size and hence “converges” towards an equidistant Simpson rule. Thus, the proposed approach is most promising for function classes that possess some structure that can be exploited.

4.1.1 Nonsmooth example: Broken Polynomial

Traditional quadrature rules and adaptive integration algorithms have problems when dealing with discontinuous or non-smooth functions, as the theoretical foundation using Taylor series expansions is no longer valid. To study the behavior on such a problem, we consider the class of functions consisting of polynomials of degree 5 with uniformly distributed coefficients in $[-1, 1]$. The non-smoothness occurs due to the fact that when the derivative of the polynomial is exactly one at a point x , the function is set to zero for all values larger than x (cf. Figure 3 for an example).

Exploiting this structure requires the reduction of the time step as the derivative of the function approaches one in order to avoid large errors at the discontinuity. In addition, the model should learn that the function remains constant after the jump and consequently choose the largest possible time step. For this example, we chose the step sizes $\{0.05, 0.075, 0.1, 0.125, 0.15, 0.2, 0.3, 0.67\}$ and the tolerance $\text{tol} = 7.5 \times 10^{-6}$. In Figure 3 (a), we see that the desired behavior can be successfully learned: Decrease the time step before the jump, then select the maximal time step after the jump. For that particular function, the model required 15 function evaluations to integrate from -1 to 1 and achieved an average error of 1.67×10^{-4} per integration step. For comparison, an equidistant Simpson rule with 15 steps has an average error of 9.07×10^{-4} per integration step, which is worse by a factor of more than five.

Unfortunately, the false detection of discontinuities poses a challenge that requires further investigation. In that case, the model prematurely chooses the maximum possible step size which results in a very large error, cf. Figure 3b. To summarize, we see that our approach has the potential to deal with discontinuities, as—in contrast to standard quadrature rules—it is not specifically tailored to smooth functions. However, this requires that these can be detected in a sufficiently accurate manner, which is obviously highly problem-dependent. We suspect that the probability of misinterpretations can be

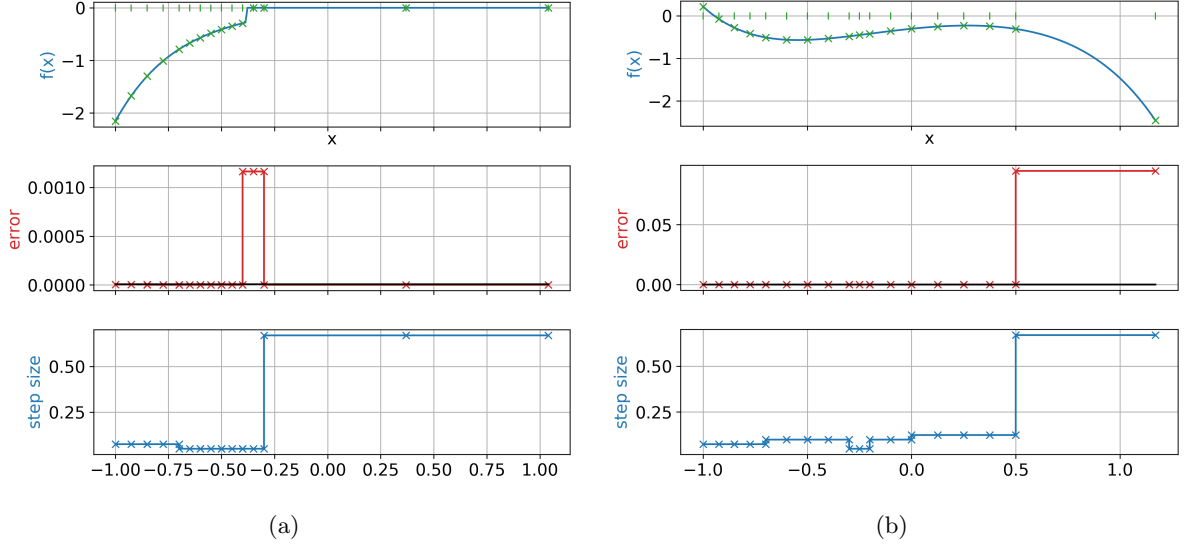


Figure 3: (a) Successful integration of a discontinuous polynomial. (b) Misinterpretation of a derivative value close to zero within the smooth domain.

reduced by using additional information (e. g., by using a memory or a model of higher order), or by using a more complex neural network to better differentiate these borderline cases.

4.2 Numerical solution of differential equations

As suggested by (3), we can extend our approach for numerical quadrature to ordinary differential equations $\dot{x} = f(t, x)$. A Runge-Kutta method with s stages can be written as

$$x(t_1) - x(t_0) = \int_{t_0}^{t_1} f(t, x(t)) dt \approx h(b_1 k_1 + \dots + b_s k_s), \quad h = t_1 - t_0.$$

The stages $k_i = f(\tilde{t}_i, \tilde{x}_i)$ correspond to approximations of the function values $f(\tilde{t}_i, x(\tilde{t}_i))$ at s different nodes $\tilde{t}_i \in [t_0, t_1]$. These are computed from internal approximations $\tilde{x}_i = x_0 + h \sum_j a_{ij} k_j$ to the values $x(\tilde{t}_i)$ of the exact solution at the nodes \tilde{t}_i . As each state k_i is allowed to depend on all other stages, the stages are determined implicitly. However, in the important special case that $a_{ij} = 0$ for $j \geq i$, the points and stages $\tilde{x}_1, k_1, \dots, \tilde{x}_s, k_s$ can be computed successively, which yields an explicit scheme. Interpreting the RK method as quadrature rules with weights $(t_1 - t_0)b_i = hb_i$ and function evaluations k_i , we adjust the input of the neural network to

$$s_t = (h, k_1, \dots, k_s). \quad (12)$$

Again, the task is to calculate an optimal step size h for the subsequent integration step by learning the Q-values for a finite set (h_1, \dots, h_n) of possible time steps. Note that the k_i are vectors with the same dimension as the state x , which we transform into a single vector in the input s_t of the NN.

The standard ODE solvers of the Python package SciPy (*RK45*) and MATLAB (*ode45*) use the Dormand-Prince pair of RK methods of order five and four, and adapt the step size based on an error estimate that is calculated using the discrepancy between the fifth and fourth order schemes. We use the same fifth order RK method in the training of the NN and compare the performance to the standard RK45 method. As before, we compare local errors (i. e., per integration step) and the number of required function evaluations.

Example 4.1 (Lorenz system). *A frequently used benchmark for ODE integrators is the chaotic Lorenz system, i. e.,*

$$\frac{d}{dt} \begin{pmatrix} x_1 \\ x_2 \\ x_3 \end{pmatrix} = \begin{pmatrix} \sigma(x_2 - x_1) \\ x_1(\rho - x_3) - x_2 \\ x_1 x_2 - \beta x_3 \end{pmatrix}, \quad x(t_0 = 0) = \begin{pmatrix} 10 \\ 10 \\ 10 \end{pmatrix},$$

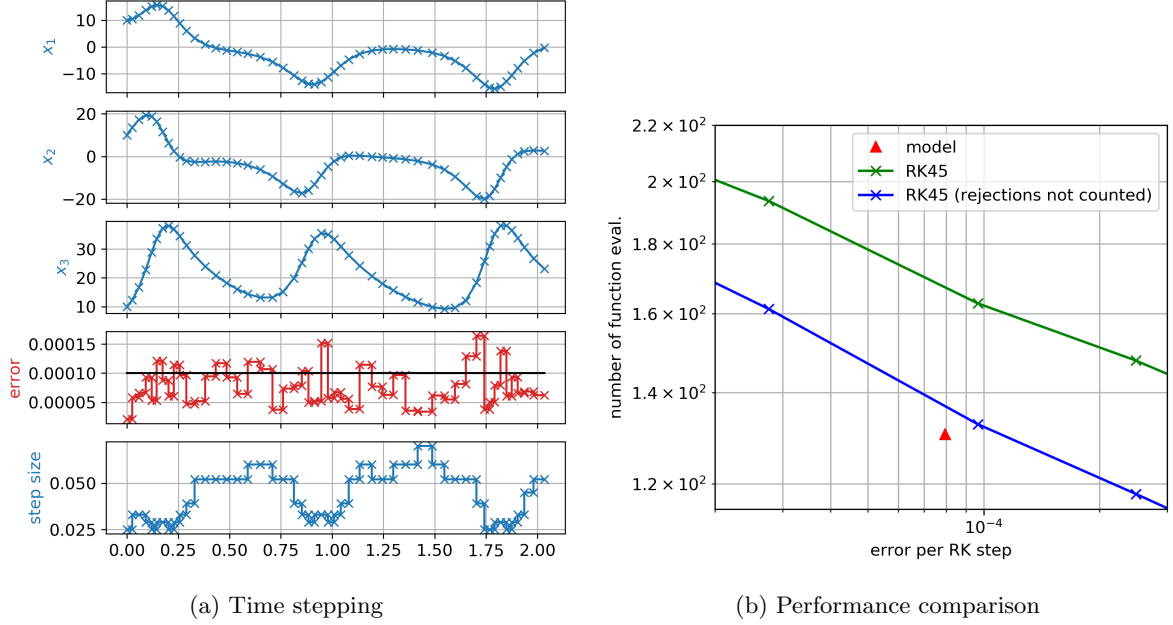


Figure 4: Lorenz System. (a) Time stepping obtained by the model. (b) Performance comparison between the model and RK45 for three different tolerances for the local error estimates.

with the standard parameter values $\sigma = 10$, $\beta = \frac{8}{3}$ and $\rho = 28$. In this regime, the system exhibits chaotic behavior. We train a single base learner with step sizes

$$h \in \{0.025, 0.029, 0.033, 0.039, 0.045, 0.052, 0.060, 0.070\},$$

a tolerance of $\text{tol} = 10^{-4}$, and the time horizon $[t_0, t_1] = [0, 200]$. Note that in contrast to the quadrature examples, we do not train the NN on an entire class of functions, but on a single ODE with a single initial condition. (The choice of a single trajectory is justified by the chaotic behavior, due to which a single trajectory yields a sufficiently rich data set.) The performance of the trained base learner is shown in Figure 4, and we see in 4b that the NN significantly outperforms RK45. Using only 130.2 function evaluations on average for a time interval of one second, the model achieves an average error of about 8×10^{-5} , while RK45 requires approximately 167.3 function evaluations to obtain the same average error. This corresponds to a reduction of the required function evaluations by approximately 22% at the same level of accuracy. As can be seen in Figure 4b, the main reason for this substantial improvement is that RK45 rejects poorly chosen time steps if the internal error estimation exceeds a certain bound. However, even without counting the rejections, the performance of our approach is slightly superior.

In a comparison for 100 random initial conditions $x_0 \sim \text{Unif}[-10, 10]^3$ instead of a single one, the NN required on average 115.1 function evaluations per time unit in comparison to 130.8 for RK45 for roughly the same average error (5.3×10^{-4}). This corresponds to a reduction of approximately 12%. To conclude, a single base learner already yields a high-performance time stepper for a smooth yet highly complex system.

Example 4.2 (Hybrid pendulum). Finally, we study a system with discontinuities in the derivatives caused by a switch in the system dynamics. We employ a meta-learner to detect these switches and choose a suitable base learner for the current situation. The system under consideration is a damped pendulum, i. e.,

$$f_1(t, x) = \begin{pmatrix} b & a \\ -a & b \end{pmatrix} x \quad \text{with } b < 0, \quad x(0) = \begin{pmatrix} 1 \\ 1 \end{pmatrix},$$

where the first coordinate x_1 refers to the position and the second coordinate x_2 to the velocity of the pendulum. After the amplitude of the oscillation falls below a certain threshold, i. e., $\|x\| < C_1$ at a previously unknown time t_1 , we quickly accelerate the pendulum, i. e., the system dynamics switches to

$$f_2(t, x) = \begin{pmatrix} 0 \\ c(t - t_1) + d \end{pmatrix}$$

until the amplitude of the system exceeds another threshold, i. e., $\|x\| > C_2 > C_1$, at time t_2 . In that case, we switch back to system f_1 , which results in a hysteresis-like system behavior; see Figure 5 for an illustration.

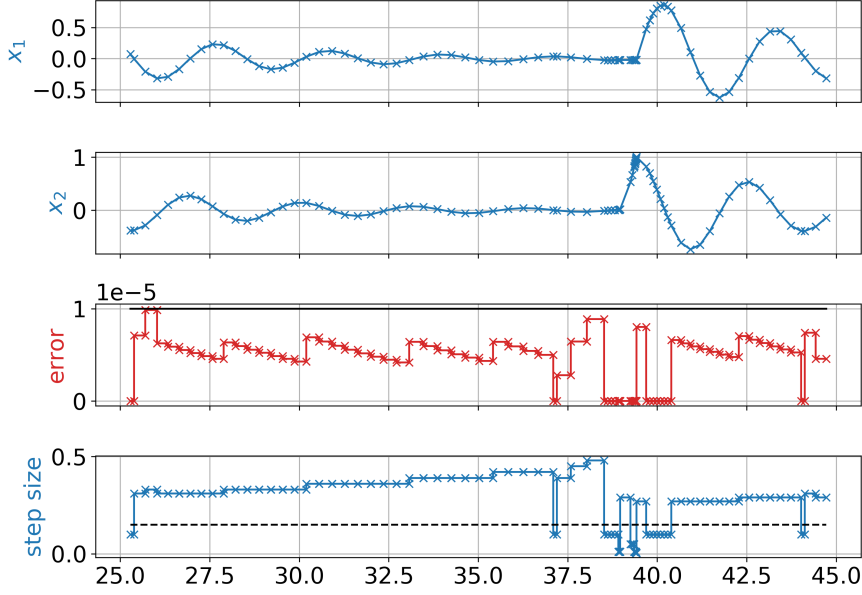


Figure 5: Adaptive integration of the hybrid pendulum using the NN-based time stepper.

We set the parameters to $a = 2$, $b = -0.2$, $c = 5$, $d = 1$ and the thresholds to $(C_1, C_2) = (0.05, 3.3)$, and begin by training a base learner for the damped system dynamics with possible step sizes

$$h \in \{0.25, 0.27, 0.29, 0.31, 0.33, 0.36, 0.39, 0.42, 0.45, 0.48\},$$

and $\text{tol} = 10^{-5}$. The training is performed using multiple runs from $x(0) = (1, 1)^\top$ until $t = t_1 \approx 20.2$. From this training, the NN successfully generalizes to the different initial conditions that arise after the switches in the system.

The other base learners from which the meta-learner can choose are trivial strategies of always picking a constant step size. For this example, we use meta-learners with constant step sizes 0.1, 0.05, 0.01, 0.005 and 0.001 in order to allow for sufficiently small step sizes at the discontinuities. This yields a total of six base learners.

To train the meta-learner, we again employ the Q-learning approach used to train the base learner, i. e., the meta-learner receives the same data to choose the optimal base learner. The selected base learner then suggests a step size which is used in the next integration step, and the resulting reward acts as feedback for the meta-learners choice.

The resulting time stepping is visualized in Figure 5. We observe that the meta-learner successfully identifies the decay process and chooses the appropriate base learners. The discontinuities are predicted correctly and small step sizes are chosen at the switching points. On average, the performance of the meta-learner and RK45 are comparable, with a slight advantage for our method. At an average error of about 1.4×10^{-5} , the NN approach requires approximately 23.9 function evaluations per time unit in comparison to 25.1 with RK45. However, in order to deal with the discontinuities, RK45 has to rely heavily on the functionality to reject poorly chosen step sizes. On average, approximately 10 steps are rejected per discontinuity.

5 Data-driven optimization of the weights and nodes of quadrature rules

Until now, we have only determined the optimal step size, with which we then performed two consecutive steps, and applied the standard Simpson's rule in (2) to determine the integral value:

$$I_i(f) = \frac{a_{i+1} - a_i}{6} \left(f(a_i) + 4f\left(\frac{a_i + a_{i+1}}{2}\right) + f(a_{i+1}) \right),$$

which can integrate polynomials up to degree three without error. Motivated by the question whether there are better choices for specific problem classes, we now again want to select optimal weights and nodes in a data-driven manner.

Let X denote a set of functions $f : [a, b] \rightarrow \mathbb{R}$ and let P be a probability measure on X . Then, we can define the integral of functions in X as the map $I : X \rightarrow \mathbb{R}$, $I(f) = \int_a^b f(x) dx$. We consider I as an element of $L_2(X, P) =: L_2$ and aim to approximate it using a set of *basis functions* $F_1, \dots, F_n \in L_2$. Typically, we would think of F_i as the evaluation at the i -th node, i. e., $F_i(f) = f(x_i)$, but other choices of basis functions could be made. Define $F := (F_1, \dots, F_n)$ and the space

$$U_F := \text{span}(F_1, \dots, F_n) \subset L_2 .$$

The scalar product on L_2 is given by $\langle F_i, F_j \rangle = \int_X F_i(f) F_j(f) dP(f) = \mathbb{E}[F_i F_j]$ and the induced norm by $\|I\|^2 = \mathbb{E}[I^2]$. We define the optimal quadrature rule $\hat{I} \in U_F$ as the element with minimal distance to the exact integral I , i. e.,

$$\hat{I} = \operatorname{argmin}_{\tilde{I} \in U_F} \|I - \tilde{I}\| .$$

Thus, \hat{I} is the best-approximation of I within U_F . As U_F is a finite-dimensional and closed subspace of L_2 , it is known that \hat{I} is uniquely determined by the orthogonal projection of I onto U_F . More precisely, $\hat{I} = \sum \omega_i F_i$ is given by the coefficients

$$\omega = A^{-1}b ,$$

where $A_{ij} = \langle F_i, F_j \rangle$ and $b_i = \langle F_i, I \rangle$. A is called *Gram* or *autocorrelation matrix* and is symmetric positive definite. We can also write the entries of A as $A_{ij} = \mathbb{E}[F_i F_j]$ and the entries of b as $b_i = \mathbb{E}[F_i I]$. We define the error of the quadrature rule as

$$\varepsilon := \|I - \hat{I}\| = \mathbb{E}[(I - \hat{I})^2]^{\frac{1}{2}} \geq \mathbb{E}[|I - \hat{I}|] =: \varepsilon_{\text{abs}} ,$$

where the inequality follows from Hölder's inequality. Thus, the error is a measure for the expected quadratic discrepancy between the quadrature rule and the exact integral, and is an upper bound for the expected absolute difference ε_{abs} .

Example 5.1 (Three Nodes). *Assume we have the three nodes x_1, x_2, x_3 and the three corresponding basis functions $F_i(f) = f(x_i)$. Then, the optimal weights $\omega = (\omega_1, \omega_2, \omega_3)$ are given by*

$$\begin{pmatrix} \mathbb{E}[F_1 F_1] & \mathbb{E}[F_1 F_2] & \mathbb{E}[F_1 F_3] \\ \mathbb{E}[F_2 F_1] & \mathbb{E}[F_2 F_2] & \mathbb{E}[F_2 F_3] \\ \mathbb{E}[F_3 F_1] & \mathbb{E}[F_3 F_2] & \mathbb{E}[F_3 F_3] \end{pmatrix} \begin{pmatrix} \omega_1 \\ \omega_2 \\ \omega_3 \end{pmatrix} = \begin{pmatrix} \mathbb{E}[F_1 I] \\ \mathbb{E}[F_2 I] \\ \mathbb{E}[F_3 I] \end{pmatrix} .$$

Thus, the optimal quadrature rule is determined by three characteristic integrals. For example, if a function f has the values $\mathbb{E}[F_1 F_1], \mathbb{E}[F_1 F_2], \mathbb{E}[F_1 F_3]$ at the nodes x_1, x_2, x_3 , then the optimal estimation for the integral is $\mathbb{E}[F_1 I]$.

Example 5.2 (One Node). *In the very basic situation where we only use a single node x_1 and the basis function $F(f) = F_1(f) = f(x_1)$, the optimal weight is $\omega = \mathbb{E}[FI]/\mathbb{E}[F^2]$ and*

$$\varepsilon^2 = \mathbb{E}[(I - \omega F)^2] = \mathbb{E}[I^2] - 2\omega \mathbb{E}[FI] + \omega^2 \mathbb{E}[F^2] = \mathbb{E}[I^2] - \frac{\mathbb{E}[FI]^2}{\mathbb{E}[F^2]} .$$

In this simple example, we can actually calculate the optimal weight for certain classes of functions. Let us for instance examine the polynomials of degree 2, i. e.,

$$X = \{f : f(x) = Ax^2 + Bx + C \mid A, B, C \in \mathbb{R}\} ,$$

with probability measure P such that A, B, C are i.i.d. with $\mathbb{E}[A] = 0$ and $\text{Var}(A) = 1$. We want to integrate from 0 to 1, i. e., $I(f) = \int_0^1 f(x) dx = \frac{1}{3}A + \frac{1}{2}B + C$. Then,

$$\begin{aligned} \mathbb{E}[F^2] &= \mathbb{E}[(Ax_1^2 + Bx_1 + C)^2] = x_1^4 \mathbb{E}[A^2] + x_1^2 \mathbb{E}[B^2] + \mathbb{E}[C^2] = x_1^4 + x_1^2 + 1 , \\ \mathbb{E}[FI] &= \mathbb{E}[(Ax_1^2 + Bx_1 + C)(\frac{1}{3}A + \frac{1}{2}B + C)] = \frac{1}{3}x_1^2 \mathbb{E}[A^2] + \frac{1}{2}x_1 \mathbb{E}[B^2] + \mathbb{E}[C^2] \\ &= \frac{1}{3}x_1^2 + \frac{1}{2}x_1 + 1 . \end{aligned}$$

Therefore, the optimal weight is

$$\omega(x_1) = \frac{\frac{1}{3}x_1^2 + \frac{1}{2}x_1 + 1}{x_1^4 + x_1^2 + 1},$$

and for the error we obtain

$$\varepsilon^2 = \mathbb{E}[I^2] - \frac{\mathbb{E}[FI]^2}{\mathbb{E}[F^2]} = \frac{49}{36} - \frac{(\frac{1}{3}x_1^2 + \frac{1}{2}x_1 + 1)^2}{x_1^4 + x_1^2 + 1}.$$

As we can now calculate the lowest possible error as a function of x_1 , we can also determine the optimal node. Here, the lowest possible error is $\varepsilon^2 \approx 0.003$, which is achieved at $x_1 \approx 0.547$ and the corresponding optimal weight is $\omega \approx 0.989$. The physical interpretation of having $x_1 > 0.5$ (instead of $x_1 = 0.5$, as one may expect) is that the function class of interest carries more “weight” on the right half of the interval $[0, 1]$.

For more general function classes and a larger number of nodes, we can approximate the optimal weights from data using linear regression. We sample functions f^j from X and collect the values $F_1(f^j), \dots, F_n(f^j)$ and $I(f^j)$. (If the exact integral is not known, we again use a composite Simpson rule with small step size.) We then solve the problem of minimizing the squared error

$$\min_{\omega} \sum_j \left(\sum_{i=1}^n \omega_i F_i(f^j) - I(f^j) \right)^2,$$

which in the infinite data limit reduces to $\omega = A^{-1}b$ as described in Example 5.1.

In the following examples, we compare this approach to the standard Newton-Cotes formulae.

Example 5.3 (Polynomials). *We first study polynomials of degree 4, 5 and 6 with $\mathcal{N}(0, 1)$ distributed coefficients. We integrate over the interval $[0, 1]$ using the equidistant nodes $[0, 0.5, 1]$. We sample 100 000 polynomials, calculate the optimal weights and compare the resulting quadrature rule to Simpson rule (i. e., $\omega = (1/6, 2/3, 1/6)$) in Table 1, where we observe a significant improvement for this non-symmetric problem class. The results are in alignment with Example 5.2 in that it is advantageous to put more weight on the right half of the interval.*

Table 1: Simpson rule versus regression-based weights for polynomials on $[0, 1]$.

degree	weights ω	ε model	ε Simpson	ε_{abs} model	ε_{abs} Simpson
4	(0.159, 0.679, 0.162)	0.0034	0.0048	0.0027	0.0042
5	(0.148, 0.698, 0.155)	0.0080	0.0129	0.0065	0.0110
6	(0.135, 0.717, 0.148)	0.0137	0.0236	0.0111	0.0195

Example 5.4 (Damped Oscillator). *The position and velocity of a damped oscillator are described by*

$$\begin{aligned} s(t) &= A \sin(\omega t + \phi) e^{-Dt}, \\ v(t) &= -Ae^{-Dt} (D \sin(\omega t + \phi) - \omega \cos(\omega t + \phi)), \end{aligned}$$

where A is the amplitude, ω the angular frequency, ϕ a phase shift, and D the damping. The objective for this example is to find the optimal quadrature rule to recover the covered distance from time $t = 0$ to $t = 1$, i. e., $s(1) - s(0) = \int_0^1 v(t) dt$, given the velocity data $(v(0), v(0.5), v(1))$. We consider oscillators with $A \in [0, 1]$, $\omega \in [0, 2\pi]$, $\phi \in [0, 2\pi]$ and $D \in [0, 1]$ due to physical limitations, and thus equip X with the probability measure P where we draw these quantities uniformly from the respective intervals. The results from sampling 100 000 velocity functions from this space and computing the optimal weights as outlined above are shown in Table 2. We again observe superior performance, which, as before, is likely due to the fact that v is not symmetric on $[0, 1]$.

Table 2: Simpson rule versus regression-based weights for the damped oscillator.

weights	ε model	ε Simpson	ε_{abs} model	ε_{abs} Simpson
(0.257, 0.624, 0.257)	0.0792	0.2281	0.0505	0.1027

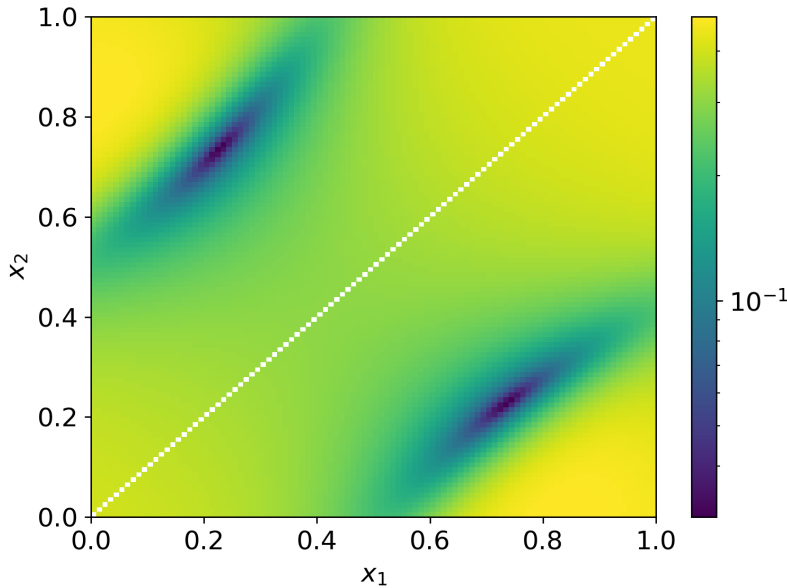


Figure 6: Error two nodes in the example of the damped oscillator.

Further experiments (for instance, on Gaussian processes) exhibit similar behavior. To summarize, the optimization of quadrature rules using linear regression is a simple technique to significantly reduce the quadrature error for non-symmetric data. In the example of the damped oscillator, we could reduce the expected absolute error in comparison to Simpson rule by 50%. A further, yet more data-intensive, step could be to use neural networks instead of linear regression to approximate optimal quadrature weights, which could result in better (though nonlinear) quadrature rules.

Remark 5.5 (Finding Optimal Nodes). *Finally, we briefly discuss the problem of finding the optimal n nodes x_1, \dots, x_n , i.e., the nodes for which the lowest possible error is achieved. The problem of choosing the corresponding optimal basis functions F_i can be seen as a problem of feature selection, which is a common task in the field of machine learning. In the case of a single node, this task can again be solved using a probabilistic standpoint. However, the selection of multiple nodes is more challenging. Figure 6 shows a grid evaluation of node positions for the damped oscillator from Example 5.4 with weights ω that have been optimized over 10 000 sample functions for these specific positions.*

A straightforward approach used for many other approximation problems is to employ sparse linear regression algorithms [28, 1], which simultaneously choose a good subset of n nodes from a larger set of nodes to choose from and calculate the optimal weights for this choice. To this end, we investigated the following algorithms (implemented in scikit-learn [18]): 1) Least absolute shrinkage and selection operator (LASSO), 2) Orthogonal Matching Pursuit, and 3) Recursive Feature Elimination. Unfortunately, none of these were able to calculate the optimal set of nodes in our examples.

Another approach is to use a general nonlinear optimization algorithm to search for the optimal set of nodes in continuous space. A disadvantage here is that we need to calculate the optimal weights and approximate the error in every step of the minimization, as the algorithm will take some unknown path through the search space. Thus, we need to sample new data for the nodes suggested by the algorithm. Although requiring a large amount of data and sampling steps, this strategy was successful in our examples.

6 Conclusion

The hierarchical reinforcement learning strategy we present for adaptive time step selection has shown great potential for both the numerical approximation of integrals and the solution of differential equations. As several examples show, state-of-the-art numerical procedures could be outperformed in both cases. While a single base learner is sufficient for smooth problems, meta-learning is particularly suited for non-smooth or hybrid systems, where sudden changes occur that can be detected and addressed by choosing a particularly suited base learner. This hierarchical approach has the advantage that the base learners may

be trained very efficiently for a well-described problem class, without the need to generalize on highly complex problems.

First experiments on the optimal choice of not only the time stepping, but also the associated weights, suggest a great potential for further improvement. For future work, it will thus be very interesting to further study and develop frameworks for the simultaneous selection of both time steps and quadrature weights. Finally, the selection of local time steps in the numerical solution of partial differential equations may also reveal further potential for performance improvements.

Code

The code is freely accessible under <https://github.com/lueckem/quadrature-ML>.

References

- [1] K. Bieker, B. Gebken, and S. Peitz. On the Treatment of Optimization Problems with L1 Penalty Terms via Multiobjective Continuation. *arXiv:2012.07483*, 2020.
- [2] S. L. Brunton, J. L. Proctor, and J. N. Kutz. Discovering governing equations from data by sparse identification of nonlinear dynamical systems. *Proceedings of the National Academy of Sciences*, 113(15):3932–3937, 2016.
- [3] P. Deuffhard and F. Bornemann. *Scientific computing with ordinary differential equations*, volume 42. Springer Science & Business Media, 2012.
- [4] P. Deuffhard and A. Hohmann. *Numerical Analysis in Modern Scientific Computing*. Springer New York, 2003.
- [5] J. Dormand and P. Prince. A family of embedded runge-kutta formulae. *Journal of Computational and Applied Mathematics*, 6(1):19 – 26, 1980.
- [6] J. Fan, Z. Wang, Y. Xie, and Z. Yang. A theoretical analysis of deep q-learning. In A. M. Bayen, A. Jadbabaie, G. Pappas, P. A. Parrilo, B. Recht, C. Tomlin, and M. Zeilinger, editors, *Proceedings of the 2nd Conference on Learning for Dynamics and Control*, volume 120 of *Proceedings of Machine Learning Research*, pages 486–489, The Cloud, 10–11 Jun 2020. PMLR.
- [7] X. Glorot and Y. Bengio. Understanding the difficulty of training deep feedforward neural networks. In Y. W. Teh and M. Titterton, editors, *Proceedings of the Thirteenth International Conference on Artificial Intelligence and Statistics*, volume 9 of *Proceedings of Machine Learning Research*, pages 249–256, Chia Laguna Resort, Sardinia, Italy, 13–15 May 2010. PMLR.
- [8] E. Hairer, C. Lubich, and G. Wanner. *Geometric Numerical Integration: Structure-Preserving Algorithms for Ordinary Differential Equations*. Springer Series in Computational Mathematics. Springer Berlin Heidelberg, 2013.
- [9] E. Hairer and G. Wanner. *Solving Ordinary Differential Equations II*. Springer Berlin Heidelberg, 1996.
- [10] E. Hairer, G. Wanner, and S. P. Nørsett. *Solving Ordinary Differential Equations I*. Springer Berlin Heidelberg, 1993.
- [11] M. J. Kearns and S. P. Singh. Finite-sample convergence rates for q-learning and indirect algorithms. In *Advances in neural information processing systems*, pages 996–1002, 1999.
- [12] D. P. Kingma and J. Ba. Adam: A method for stochastic optimization. *arXiv:1412.6980*, 2014.
- [13] S. Klus, F. Nüske, S. Peitz, J.-H. Niemann, C. Clementi, and C. Schütte. Data-driven approximation of the Koopman generator: Model reduction, system identification, and control. *Physica D: Nonlinear Phenomena*, 406:132416, 2020.
- [14] M. Knöller, A. Ostermann, and K. Schratz. A fourier integrator for the cubic nonlinear schrödinger equation with rough initial data. *SIAM Journal on Numerical Analysis*, 57(4):1967–1986, 2019.
- [15] T. P. Lillicrap, J. J. Hunt, A. Pritzel, N. Heess, T. Erez, Y. Tassa, D. Silver, and D. Wierstra. Continuous control with deep reinforcement learning. In *ICLR (Poster)*, 2016.
- [16] Y. Liu, J. Kutz, and S. Brunton. Hierarchical deep learning of multiscale differential equation time-steppers. *ArXiv*, abs/2008.09768, 2020.
- [17] V. Mnih, K. Kavukcuoglu, D. Silver, A. A. Rusu, J. Veness, M. G. Bellemare, A. Graves, M. Riedmiller, A. K. Fidjeland, G. Ostrovski, S. Petersen, C. Beattie, A. Sadik, I. Antonoglou, H. King, D. Kumaran, D. Wierstra, S. Legg, and D. Hassabis. Human-level control through deep reinforcement learning. *Nature*, 518(7540):529–533, feb 2015.

- [18] F. Pedregosa, G. Varoquaux, A. Gramfort, V. Michel, B. Thirion, O. Grisel, M. Blondel, P. Prettenhofer, R. Weiss, V. Dubourg, J. Vanderplas, A. Passos, D. Cournapeau, M. Brucher, M. Perrot, and E. Duchesnay. Scikit-learn: Machine learning in Python. *Journal of Machine Learning Research*, 12:2825–2830, 2011.
- [19] M. L. Piscopo, M. Spannowsky, and P. Waite. Solving differential equations with neural networks: Applications to the calculation of cosmological phase transitions. *Phys. Rev. D*, 100:016002, Jul 2019.
- [20] M. Raissi, P. Perdikaris, and G. E. Karniadakis. Physics informed deep learning (part i): Data-driven solutions of nonlinear partial differential equations. *arXiv:1711.10561*, 2017.
- [21] F. Regazzoni, L. Dedè, and A. Quarteroni. Machine learning for fast and reliable solution of time-dependent differential equations. *Journal of Computational Physics*, 397:108852, 2019.
- [22] S. H. Rudy, S. L. Brunton, J. L. Proctor, and J. N. Kutz. Data-driven discovery of partial differential equations. *Science Advances*, 3(4):1–6, 2017.
- [23] J. Schmidhuber. Evolutionary principles in self-referential learning. Diploma thesis, Department of Informatics, Technical University of Munich, May 1987.
- [24] SciPy. v1.5.4 reference guide: Integration and ODEs (scipy.integrate.solve_ivp). https://docs.scipy.org/doc/scipy/reference/generated/scipy.integrate.solve_ivp.html. Online; accessed 4 December 2020.
- [25] L. F. Shampine and M. W. Reichelt. The MATLAB ODE suite. *SIAM Journal on Scientific Computing*, 18(1):1–22, 1 1997.
- [26] J. Sirignano and K. Spiliopoulos. Dgm: A deep learning algorithm for solving partial differential equations. *Journal of Computational Physics*, 375:1339 – 1364, 2018.
- [27] R. S. Sutton and A. G. Barto. *Reinforcement Learning: An Introduction*. A Bradford Book, Cambridge, MA, USA, 2018.
- [28] D. Vidaurre, C. Bielza, and P. Larrañaga. A survey of L1 regression. *International Statistical Review*, 81(3):361–387, 2013.
- [29] P. Virtanen et al. SciPy 1.0: Fundamental Algorithms for Scientific Computing in Python. *Nature Methods*, 17:261–272, 2020.
- [30] C. J. C. H. Watkins and P. Dayan. Q-learning. *Machine Learning*, 8(3):279–292, May 1992.
- [31] Wolfram Research Inc. Wolfram Language & System Documentation Center: The design of the NDSolve framework. <https://reference.wolfram.com/language/tutorial/NDSolveDesign.html>. Online; accessed 4 December 2020.